



Roles of intraloops-2 and -3 and the proximal C-terminus in signalling pathway selection from the human calcium-sensing receptor



Mahvash A. Goolam^a, James H. Ward^a, Vimesh A. Avlani^a, Katie Leach^b, Arthur Christopoulos^b, Arthur D. Conigrave^{a,*}

^aSchool of Molecular Bioscience, University of Sydney, NSW 2006, Australia

^bMonash Institute of Pharmaceutical Sciences and Department of Pharmacology, Monash University, Parkville, Victoria 3052, Australia

ARTICLE INFO

Article history:

Received 10 May 2014

Revised 3 July 2014

Accepted 16 July 2014

Available online 28 July 2014

Edited by Ned Mantei

Keywords:

Calcium-sensing receptor

G-protein coupled receptor

Biased signalling

Phosphatidylinositol-specific

phospholipase-C

Adenosine 3',5'-cyclic monophosphate

ERK_{1/2}

ABSTRACT

The calcium-sensing receptor (CaSR) couples to signalling pathways via intracellular loops 2 and 3, and the C-terminus. However, the requirements for signalling are largely undefined. We investigated the impacts of selected point mutations in iL-2 (F706A) and iL-3 (L797A and E803A), and a truncation of the C-terminus (R866X) on extracellular Ca²⁺ (Ca_o²⁺)-stimulated phosphatidylinositol-specific phospholipase-C (PI-PLC) and various other signalling responses. CaSR-mediated activation of PI-PLC was markedly attenuated in all four mutants and similar suppressions were observed for Ca_o²⁺-stimulated ERK_{1/2} phosphorylation. Ca_o²⁺-stimulated intracellular Ca²⁺ (Ca_i²⁺) mobilization, however, was relatively preserved for the iL-2 and iL-3 mutants and suppression of adenylyl cyclase was unaffected by either E803A or R866X. The CaSR selects for specific signalling pathways via the proximal C-terminus and key residues in iL-2, iL-3.

© 2014 Federation of European Biochemical Societies. Published by Elsevier B.V. All rights reserved.

1. Introduction

The extracellular Ca²⁺-sensing receptor (CaSR) belongs to a nutrient-sensing receptor subgroup of G-protein-coupled receptor (GPCR) Class C (reviews: [1,2]). It conforms to a domain-based structure that includes an N-terminus extracellular Venus FlyTrap (VFT) domain linked to a canonical heptahelical signalling domain via an intervening Cysteine-rich domain (reviews: [3,4]). An extended intracellular C-terminal domain of 215 residues provides interactions between the receptor, the cytoskeleton, and some of its key signalling partners (review: [5]). The CaSR acts as a key component of the calcioostat that provides feedback regulation of parathyroid hormone secretion (review: [6]). In addition, it is expressed widely in tissues including the kidney, gastro-intestinal tract, bone, brain, and lung in which it plays quite different roles.

Abbreviations: GPCR, G-protein coupled receptor; CaSR, calcium-sensing receptor; PI-PLC, phosphatidylinositol-specific phospholipase-C; VFT, Venus FlyTrap; CR, Cysteine-rich; iL, intraloop; cAMP, adenosine 3',5'-cyclic monophosphate; pERK, phosphorylated extracellular regulated kinase; IP₁, inositol 1-phosphate

* Corresponding author. Address: School of Molecular Bioscience (G08), University of Sydney, NSW 2006, Australia. Fax: +61 2 9351 5858.

E-mail address: arthur.conigrave@sydney.edu.au (A.D. Conigrave).

These include contributions to the control of epithelial transport, hormone secretion, and even cell fate (review: [7]).

The CaSR binds and responds to various endogenous ligands including not only extracellular Ca²⁺ (Ca_o²⁺) and Mg²⁺ but also organic multivalent cations such as spermine, which acts as an allosteric agonist [8] and L-amino acids, which act as positive modulators (review: [9]) that bind in the receptor's VFT domain [10]. In addition, the CaSR is activated by synthetic modulators (calcimimetics) including the clinically effective phenylalkylamine cinacalcet, which bind in the receptor's heptahelical domain [11].

The finding that the receptor has multiple ligand binding sites and responds to multiple sensing modalities has led us to investigate whether the receptor employs ligand-biased signalling to control function in its diverse cellular contexts. Thus far, these studies have demonstrated that the CaSR exhibits pronounced ligand-biased signalling via pathways coupled to intracellular Ca²⁺ (Ca_i²⁺) mobilization, ERK_{1/2} phosphorylation and membrane ruffling [12], and that mutations associated with disturbed CaSR function in vivo perturb the normal balance between different signalling pathways with respect to the potencies and even efficacies of Ca_o²⁺ and other activators [13,14]. The findings indicate that signalling bias is an important property of the receptor that can explain

key differences in receptor function between tissues and also in the patterns of disease arising from specific disease-related mutations.

Signalling bias arises from the adoption of specific ligand-bound receptor conformations that select between signalling pathways, pointing to the existence of distinct molecular requirements for the activation of different G-proteins and their downstream signalling pathways. In response to stimulation by its principal physiological agonist, Ca_0^{2+} , for example, the CaSR couples to various intracellular signalling responses including $\text{G}_{q/11}$ -mediated activation of PI-PLC, Ca_i^{2+} mobilization, $\text{G}_{i/o}$ -mediated inhibition of adenylyl cyclase, and thus suppression of intracellular cAMP levels (review: [6]), as well as the phosphorylation of various protein kinases including the MAP kinase $\text{ERK}_{1/2}$ (p $\text{ERK}_{1/2}$) [15,16].

In the present study, we set out to investigate whether it is possible to define distinct subsets of molecular requirements for the Ca_0^{2+} -stimulated activation of $\text{G}_{q/11}$, $\text{G}_{i/o}$ and $\text{ERK}_{1/2}$ phosphorylation, taking advantage of previous work on the molecular requirements of Ca_0^{2+} -stimulated PI-PLC activation by the bovine CaSR [17], which exhibits 93% amino acid identity with the human CaSR (hCaSR). This work identified the conserved residue F707 (hCaSR residue F706) in iL-2, and three mutants homologous to hCaSR L797A, F801A and E803A, all of which exhibited marked attenuations in their Ca_0^{2+} -stimulated PI-PLC responses [17]. Furthermore, truncation of the proximal C-terminus beyond hCaSR residue S865, by the introduction of a premature stop codon R866X, abolished PI-PLC signalling [18,19].

Thus, we investigated the impacts of four human CaSR mutants on Ca_0^{2+} -stimulated signalling responses including: PI-PLC as reported by IP_1 accumulation; Ca_i^{2+} mobilization; p $\text{ERK}_{1/2}$; and suppression of adenylyl cyclase. The results indicate that there are distinct G-protein coupling requirements for CaSR-mediated $\text{G}_{q/11}$ and $\text{G}_{i/o}$ activation and that these differences are important for signalling pathway selection in response to elevated Ca_0^{2+} . Since distinct ligands exhibit significant differences in CaSR-mediated signalling pathway selection the current findings would also appear to provide insights into the nature of biased signalling responses.

2. Materials and methods

2.1. Construction of mutant receptors

The wild-type (WT) human CaSR cDNA (cassette version, [20]) cloned between the *Kpn* I and *Xba* I sites of pcDNA3.1 (+) {pcDNA3.1 (+)-WTCaSR} was a kind gift from Dr. Mei Bai and Prof. Edward Brown (Endocrine-Hypertension Division and Membrane Biology Program, Brigham and Women's Hospital, Boston, MA, USA). All mutants were generated in pcDNA3.1(+)-WTCaSR and/or pcDNA3.1(+)-WTCaSR(FLAG) plasmid, which contains the FLAG epitope DYKDDDDK between residues 371 and 372; insertion of the FLAG epitope at this position has been shown previously to have no impact on receptor function [21]. The Quikchange II site-directed mutagenesis protocol was used to introduce the point mutations F706A, L797A and E803A. Briefly, pairs of complementary or overlapping primers (30–40 bases) were designed to encode the required mutation with flanking wild-type sequences of around 15–20 bases. The template DNA was amplified for 18 cycles with Pfu Ultra II HS DNA polymerase (Agilent Technologies, USA). Following digestion with *Dpn* I, amplified DNA was transformed into DH5 α *Escherichia coli* cells. Sequences of forward and reverse primers used to generate the required point mutations are shown in Table 1.

A truncation mutant, R866X, which introduces a premature stop codon after S865 in the proximal C-terminus, was also generated. Briefly, the template cDNA was amplified by PCR using a

Table 1

Sequences of forward and reverse primers used to generate the CaSR point mutations tested in the study. The mutated codon is underlined.

Mutant	Primers used in site-directed mutagenesis reactions
F706A	F: 5'-CCAACCGTGTCTCTCTGGTGG <u>CT</u> GAGGCCAAGAT-3' R: 5'-TGGGGATCTTGGCCTCAGCCACCAGGAGGACA-3'
L797A	F: 5'-TTCAAGTCCCGGAAGG <u>CCG</u> CCGGAGAAGCTCAATGAA-3' R: 5'-AAGTTCCTCCGGCCCTCCGGGACTTGAAGGCAAA-3'
E803A	F: 5'-GCCGGAGAAGCTCAATGCAGCCAAGTTCATCACCTTCAG-3' R: 5'-GTGATGAAGTGGCTGCATTGAAGTTCCTCCGGCAGCTTC-3'

forward primer designed to bind to the first 22 nucleotides of the CaSR cDNA with a 5' *Kpn* I site (5'-CAG TAT GGT ACC ATG GCA TTT TAT AGC TGC TGC T) and a reverse primer (5'-TAGACT TCT AGA TTA GGA TGG CTT GAA GAG AAT GAT) that introduced a stop codon (TAA) at residue 866 (underlined) followed by a 3' *Xba* I site. The PCR product obtained using the wild-type CaSR as the template was digested with *Kpn* I and *Xba* I and ligated into the multiple cloning site of purified pcDNA3.1(+) that had been pre-digested using these enzymes. The identities of all completed mutants were confirmed by DNA sequencing (Australian Genome Research Facility, Sydney, NSW, Australia).

2.2. Cell culture and transfection

HEK-293 cells were cultured in Dulbecco's modified Eagle medium (DMEM) supplemented with 10% FBS, 25 Units/ml Penicillin and 25 $\mu\text{g}/\text{ml}$ Streptomycin, and maintained at 37 °C in a humidified 5% CO_2 incubator. When cells had reached 85–95% confluency they were transfected with XtremeGENE HP transfection reagent (Roche, Germany). Briefly, 0.5–1 μg samples of WT or mutant DNA in 1–2 μl of water and 3 μl of transfection reagent were diluted with 100 μl of DMEM and allowed to complex at RT for 15 min. The transfection solution was added to the cell cultures to a final concentration of 9.1% (v/v). In all experimental series, identical DNA concentrations were used for all constructs tested (i.e., WT and all four mutants). For cAMP measurements, 0.5 μg samples of cAMP reporter construct DNA were added along with the WT or mutant DNA to the transfection solutions.

2.3. Quantitation of total and surface receptor expression

HEK-293 cells were cultured in 96-well poly-D-lysine coated plates and transiently transfected for 48 h with either the wild-type CaSR or one of several mutant CaSRs. After transfection, cell samples, at an approximate density of 100% (4×10^4 cells well $^{-1}$), were washed once with TBS-T (0.05 M Tris, 0.15 M NaCl, 0.05% (v/v) Tween-20, pH 7.4) and fixed for 15 min on ice with either 4% (w/v) paraformaldehyde in PBS (137 mM NaCl, 2.7 mM KCl, 10 mM Na_2HPO_4 , 1.8 mM KH_2PO_4 , pH 7.4) to determine surface expression, or methanol, to determine total cell expression. All subsequent steps were performed at room temperature. After washing once with TBS-T, fixed cell samples were incubated with 1% (w/v) skim milk solution in TBS-T for 1 h and then incubated with monoclonal anti-FLAG M2 horse-radish peroxidase (HRP)-conjugated antibody (Sigma Aldrich #A8592) diluted 1:5000 in TBS-T for 1 h. The wells were then washed three times with PBS and incubated with the HRP substrate, 3,3',5,5' tetramethylbenzidine liquid substrate solution (Sigma Aldrich cat. #T0440) in the dark for 12 min. Enzyme reactions were stopped by the addition of equal volumes of 1 M HCl. Supernatant samples were transferred to new 96-well plates and A_{450} values were obtained using a Perkin-Elmer EnVision 2103 multilabel counter (software version 1.08, Perkin Elmer, USA).

2.4. Homogeneous time-resolved fluorescence assay for inositol monophosphate (IP₁)

HEK-293 cells were cultured in 6-well plates and transfected at 90% confluency for 24 h. Cell samples (from ca. 1.2×10^6 cells) were detached with 0.2 ml lots of 0.25% trypsin–EDTA, followed by the addition of 5–10 ml DMEM (10% FBS; 25 Units/ml Penicillin, 25 µg/ml Streptomycin) and centrifugation (210×g, 3 min). Cell pellets were re-suspended in 1.2 ml of DMEM (10% FBS, 25 Units/ml Penicillin, 25 µg/ml Streptomycin), and 30 µl samples of cell suspensions were aliquoted into 384 well Optiplates (Perkin Elmer, USA) and cultured for 24 h. On the day of the experiment, the medium was removed from each well and the cells were incubated for 30 min in 14 µl lots of stimulation buffer that contained 146 mM NaCl, 4.2 mM KCl, 5.5 mM glucose, 0.5 mM MgCl₂, 10 mM HEPES (pH 7.4), and 50 mM LiCl to suppress IP₁ breakdown. IP₁ was detected by overnight incubation with 3 µl/well of anti-IP₁ cryptate Tb conjugated antibody (diluted in 1 × lysis buffer according to the manufacturer's instructions) and 3 µl/well of similarly prepared IP₁-d2 conjugate. Time-resolved FRET was measured on a Perkin-Elmer EnVision 2103 multilabel counter with excitation at 320 nm and emission at 615 and 665 nm. The F₆₁₅/F₆₆₅ emission ratio was used as a measure of IP₁.

2.5. Cytoplasmic Ca²⁺ mobilization fluorescence assay

Microfluorimetry to measure changes in Ca_i²⁺ was performed as described previously [22]. All Ca²⁺ solutions were prepared in physiological saline solution (PSS) that contained 125 mM NaCl, 4 mM KCl, 0.1% (w/v) D-Glucose, 1 mM MgCl₂, 20 mM HEPES (pH 7.45 adjusted with NaOH). Briefly, HEK-293 cells that had been cultured on 15 mm sterile glass coverslips in 24-well plates were transfected with either the WTCaSR or one of several CaSR mutants for 48 h. After transfection, the cells were rinsed with PSS supplemented with 0.8 mM NaH₂PO₄ and 0.1% (w/v) bovine serum albumin (BSA) and then incubated with this solution containing 5 µM Fura 2-AM for 90–120 min at 37 °C in a humidified 5% CO₂ incubator in the dark. The cells were washed once and stored in loading solution until required for microscopy.

For microfluorimetry, cells on coverslips that had been loaded with Fura 2-AM were placed in a closed bathing chamber and mounted onto the stage of a Zeiss Axiovert 200 M fluorescence microscope for live cell imaging and perfused with PSS containing various Ca_o²⁺ concentrations. Fluorescence images were obtained using a 63× objective following excitation from a Lambda DG-4 Xenon light source (Sutter) at alternating wavelengths of 340 and 380 nm with an exposure time of 0.5 s. Images were collected via an emission filter centred on 510 nm using an Axiocam HSm digital camera (Zeiss) and downloaded using Slidebook software (Intelligent Imaging Solutions; Colorado, USA). F₃₄₀/F₃₈₀ excitation ratio data were used as measures of Ca_i²⁺ concentration and integrated to assess Ca_o²⁺ concentration-dependent responses. The data were expressed as integrated fluorescence response units (IFRUs) and normalised with respect to the responses for control Ca_o²⁺ (0.5 mM) as required.

2.6. AlphaScreen ERK_{1/2} phosphorylation assay

Receptor-mediated ERK_{1/2} phosphorylation was quantified using AlphaScreen SureFire assays (Perkin Elmer, USA). HEK-293 cells were seeded onto poly-D-lysine coated 96-well plates and transfected with the WTCaSR or one of the CaSR mutants for 48 h as needed. After transfection, the cells were pre-incubated at 37 °C in a humidified 5% CO₂ incubator for 4–14 h in DMEM/0.2% BSA (no FBS) that contained 1.5 mM Ca²⁺. Serum starvation between these time intervals had the effect of lowering

background levels of pERK_{1/2} due, presumably, to the withdrawal of serum growth factors. The medium was then removed from each well and after washing with PSS (0.2 ml), the cells were pre-incubated in PSS that contained 0.2 mM Ca²⁺ (90 µl) for 30 min. The wells containing adherent cells were then activated by the addition of 10 µl lots of PSS that contained 10× final Ca²⁺ concentration for 10 min at 37 °C. The supernatants were then removed and the cells were lysed by the addition of 50 µl lots of AlphaScreen Lysis Buffer (Perkin-Elmer) with shaking at 150 rpm for 10–15 min at RT. Samples of lysates (5 µl lots) were then transferred to 384-well Optiplates (Perkin-Elmer) and incubated overnight with acceptor and donor beads as specified in the manufacturer's instructions. Chemiluminescence counts were quantified using the AlphaScreen protocol in a Perkin-Elmer EnVision 2103 multilabel counter. To generate Ca_o²⁺ concentration–response curves, raw data were expressed as fold-changes with respect to the behaviour of the WT CaSR at baseline Ca_o²⁺ (0.5 mM).

2.7. Intracellular cAMP assay

Microfluorimetry was performed to detect changes in intracellular cAMP levels as described previously [22]. Briefly, HEK-293 cells were seeded onto sterile glass coverslips in 24-well plates. The cells were then transfected with either the WTCaSR, or one of several mutant CaSR constructs, and co-transfected with the cAMP fluorescence resonance energy transfer reporter construct: CFP-EPAC-YFP-YFP (the kind gift of Dr. Kees Jalink, Netherlands Cancer Institute [23]). After 48 h, the medium was removed from each well and the cells were incubated with 0.5 mM Ca²⁺ in PSS for 15 min at 37 °C. The coverslips were then transferred individually to a closed bathing chamber and placed in the light path of the Zeiss Axiovert 200 M microscope described above. The cells were then exposed to PSS that contained 1 µM Forskolin for 15 min to elevate intracellular cAMP levels in the presence of baseline Ca_o²⁺ (0.5 mM) followed by stepwise increments in Ca_o²⁺ (0.5–10 mM) for 7 min each. In control experiments, 7 min was found to be an appropriate time for the adoption of a new steady-state level of cAMP. Excitation was performed at a constant wavelength of 436 nm and emission was performed at alternating wavelengths of 488 and 528 nm for intervals of 0.5 s corresponding to F_{CFP} and F_{YFP}, respectively. Images were collected using the Axiocam HSm digital camera described above in Section 2.5 and computed by Slidebook software as the F_{CFP}/F_{YFP} emission ratio as a measure of intracellular cAMP levels. The emission ratios arising from the last one-minute intervals of exposure were averaged and after background subtraction (0.5 mM Ca_o²⁺ control) were expressed as percentages of the Forskolin-stimulated emission ratio to generate Ca_o²⁺ concentration–response curves.

2.8. Curve fitting and statistical analysis

The data are expressed routinely as means ± S.E.M. For Ca_i²⁺ mobilization experiments, Ca_o²⁺ concentration–response data were obtained by integrating the F₃₄₀/F₃₈₀ excitation ratio data obtained in response to each Ca_o²⁺ concentration as described previously [22]. Concentration–response data for IP₁ accumulation, Ca_i²⁺ mobilization and pERK_{1/2} were fitted to the following form of the Hill equation:

$$R = d + (a - d) \cdot C^b / (e^b + C^b) \quad (1)$$

where a = maximal response (E_{\max}); b = Hill co-efficient; e = half maximal effective concentration (EC_{50}); d = minimum response. Concentration–response data for suppression of intracellular cAMP levels were fitted using the following equation:

$$R = a - (a - d) \cdot C^b / (e^b + C^b) \quad (2)$$

where the parameters a , b , d , and e have the same meanings as in Eq. (1).

Statistical analyses were performed using analysis of variance (ANOVA) in GraphPad Prism 5. Statistical significance was accepted at $P < 0.05$. Log transformations of EC_{50} or IC_{50} values were used to assess the statistical significance of differences in Ca_o^{2+} -sensitivity.

3. Results

3.1. Construction and expression of PLC signalling defective CaSR mutants

To assess the impacts of the PI-PLC-signalling defective mutants on various CaSR-mediated signalling pathways, we generated three alanine mutants in CaSR iL-2 (F706A) and iL-3 (L797A and E803A) as well as a C-terminus truncation mutant, R866X, which retains only the three membrane-proximal residues (863–KPS–865) of the normal 216 residue C-terminus (Fig. 1A). The constructs were transiently transfected into HEK-293 cells to assess expression and function. Levels of total and cell surface expression for all four

mutants were comparable to WT as determined by anti-FLAG antibody-based ELISAs (Fig. 1B).

3.2. The impacts of iL-2, iL-3 and C-terminus truncation mutants on CaSR-mediated IP_1 accumulation

The PI-PLC signalling properties of the mutants were assessed by IP_1 accumulation in transiently-transfected HEK-293 cells exposed to stepwise increases in Ca_o^{2+} in the range 0.5–20 mM (Fig. 2A). A homogeneous time-resolved FRET (HTRF)-based competitive assay was used to assess IP_1 levels over 30 min. WTCaSR transfected HEK-293 cells responded to elevated Ca_o^{2+} with increased IP_1 accumulation and a maximally effective Ca_o^{2+} of 20 mM; a 4-fold increase in IP_1 was observed with respect to the baseline response at 0.5 mM Ca_o^{2+} .

All mutant CaSR-expressing cells exhibited markedly impaired IP_1 responses that were significantly reduced at 20 mM Ca_o^{2+} compared to WT ($P < 0.0001$; 2-way ANOVA). The maximal responses of HEK-293 cells expressing E803A and R866X were around 30%, and the maximal responses of HEK-293 cells expressing F706A and

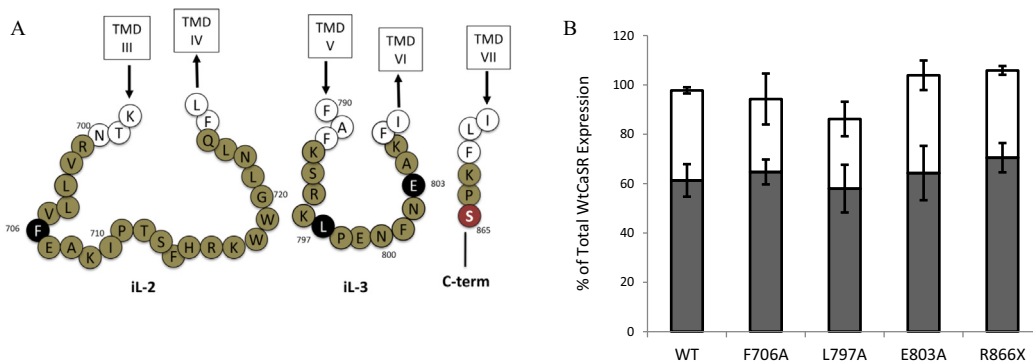


Fig. 1. PI-PLC signalling-defective mutants in iL-2, iL-3 and the C-terminal region, and their impact on receptor expression. (A) The residues that were mutated are shown in black in both iL-2 (F706) and iL-3 (L797 and E803). A mutation (R866X) that truncates the C-terminal region after S865 (red) was also generated. All four mutants have been reported previously to impair PI-PLC signalling [17,19]. (B) Effects of iL point mutations and a C-terminus truncation mutant on CaSR total and surface expression. HEK-293 cells were transiently transfected with FLAG-tagged WT or mutant constructs, and then fixed and probed with anti-FLAG antibody to measure total ($\square + \blacksquare$) or cell surface expression (\blacksquare) as described in the Section 2. Results obtained in HEK-293 cells transfected with vector alone were used for background subtraction and the results for all mutants were normalised to the level of total WTCaSR expression. The results were obtained in four independent experiments.

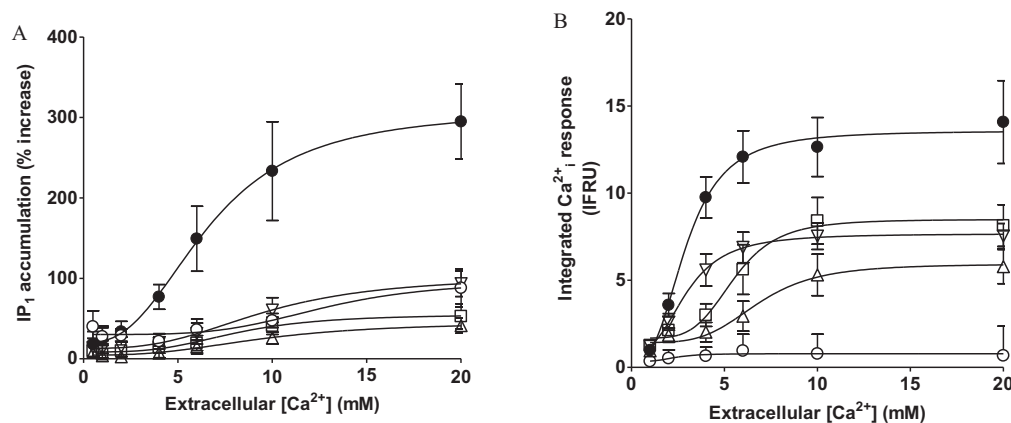


Fig. 2. Impact of CaSR mutants on Ca_o^{2+} -stimulated IP_1 accumulation and Ca_i^{2+} mobilization. HEK-293 cells were transiently transfected with the WTCaSR (●), or one of several CaSR mutants including R866X (○), F706A (□), L797A (△), or E803A (▽). In (A), they were exposed to various Ca_o^{2+} concentrations prior to lysis, and then processed for IP_1 accumulation as described in the Section 2 (4–5 independent experiments). In (B), transfected cells that had been grown on coverslips were loaded with fura-2 AM and mounted in a perfusion chamber in the light path of a Zeiss Axiocvert microscope for live cell imaging, after which they were exposed to step-wise increments in Ca_o^{2+} from 0.5 to 20 mM. F_{340}/F_{380} excitation ratio data were integrated to allow the generation of concentration–response curves (9–10 cells in each of 4–9 independent experiments).

L797A were around 15–20% of WT. The results were comparable to those described previously [17,19].

3.3. The impacts of iL-2, iL-3 and C-terminus truncation mutants on CaSR-mediated Ca_i^{2+} mobilization

We next investigated the impacts of the mutants on Ca_i^{2+} mobilization in single Fura 2- loaded HEK-293 cells by microfluorimetry. The WTCaSR induced Ca_o^{2+} -dependent Ca_i^{2+} mobilization with an EC_{50} for Ca_o^{2+} of 2.9 ± 0.2 mM and an E_{max} of 13.8 ± 0.4 IFRU, and the C-terminus truncation mutant R866X abolished Ca_o^{2+} -dependent Ca_i^{2+} mobilization (Fig. 2B). In the cases of all three iL point mutants studied, however, Ca_i^{2+} mobilization was relatively preserved. Thus, there were only approximately 50% reductions in E_{max} values (all $P < 0.01$) and the EC_{50} values for Ca_o^{2+} were similar to and not significantly different from WT ($P > 0.1$ in all cases; Fig. 2B). In particular, the EC_{50} values for Ca_o^{2+} in the case of the iL-2 mutant F706A was 5.3 ± 0.6 mM and in the cases of the iL-3 mutants L797A and E803A were 6.8 ± 1.4 and 3.0 ± 0.6 mM respectively. Thus, the impacts of the iL-2 and iL-3 mutants were less marked on Ca_i^{2+} mobilization than on IP_1 accumulation, although Ca_i^{2+} mobilization was abolished in HEK-293 cells that were transiently transfected with R866X.

3.4. The impacts of iL-2, iL-3 and C-terminus truncation mutants on CaSR-mediated phosphorylation of $\text{ERK}_{1/2}$

The impacts of the mutants on Ca_o^{2+} -stimulated $\text{ERK}_{1/2}$ phosphorylation (p $\text{ERK}_{1/2}$) were investigated using a dual antibody AlphaScreen assay as described in the Section 2. In HEK-293 cells expressing the WTCaSR, elevated Ca_o^{2+} induced concentration-dependent increases in p $\text{ERK}_{1/2}$ to a maximum 10–12-fold above the baseline level observed at a Ca_o^{2+} of 0.5 mM. The EC_{50} for Ca_o^{2+} was 2.4 ± 0.3 mM (Fig. 3). The C-terminus truncation mutant did not support Ca_o^{2+} -stimulated p $\text{ERK}_{1/2}$ at concentrations up to 10 mM. In addition, the three point mutations F706A, L797A and E803A markedly suppressed the E_{max} values by $\geq 90\%$ with respect to the WTCaSR ($P < 0.001$ in all three cases). The results indicate that Ca_o^{2+} -stimulated CaSR-mediated p $\text{ERK}_{1/2}$ is critically dependent on residues in iL-2 and iL-3 that are required for PI-PLC activation along with residues that lie to the C-terminus side of S865.

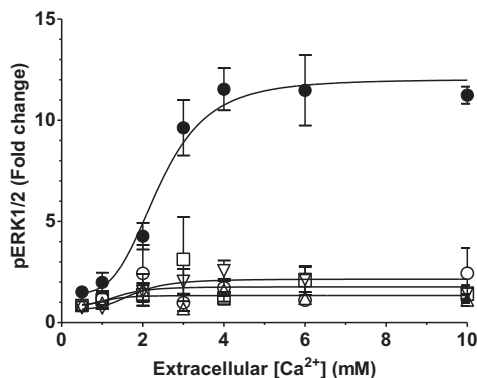


Fig. 3. Impact of CaSR mutants on Ca_o^{2+} -stimulated p $\text{ERK}_{1/2}$. $\text{ERK}_{1/2}$ phosphorylation levels in cell lysates prepared from HEK-293 cells that had been first transfected with the WTCaSR (●), or one of several mutants including R866X (○), F706A (□), L797A (△) or E803A (▽), and then exposed to various Ca_o^{2+} concentrations for 10 min, were quantified using the AlphaScreen p $\text{ERK}_{1/2}$ assay as described in the Section 2. The results are expressed relative to HEK-293 cells transfected with WTCaSR and exposed to baseline Ca_o^{2+} (0.5 mM). The results were obtained in 3–8 independent experiments.

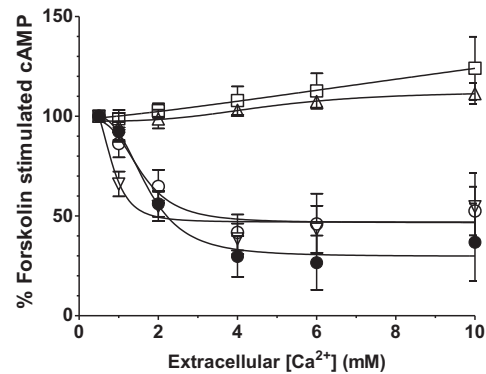


Fig. 4. Impact of iL-2, iL-3 mutations and C-terminus truncation on Ca_o^{2+} -stimulated suppression of forskolin-stimulated cAMP levels. HEK-293 cells were co-transfected with a FRET-Epac reporter construct and either the WTCaSR (●) or one of several CaSR mutants including R866X (○), F706A (□), L797A (△), or E803A (▽). The cells were then exposed to 1 μM forskolin at baseline Ca_o^{2+} (0.5 mM) followed by step-wise increments in Ca_o^{2+} from 0.5 to 10 mM. The results were obtained from single cells by microfluorimetry and normalized to control the cAMP level induced by 1 μM forskolin, as described in the Section 2. The results were obtained in 8–10 cells in each of three independent experiments.

3.5. The impacts of iL-2, iL-3 and C-terminus truncation mutants on CaSR-mediated suppression of adenylyl cyclase as reported by cAMP levels

We next examined the impacts of the iL-2, iL-3 and C-terminus truncation mutants on CaSR-mediated suppression of adenylyl cyclase as reported by cAMP levels measured in individual cells by microfluorimetry. Initial experiments demonstrated that Ca_o^{2+} -dependent suppression of intracellular cAMP levels but not Ca_o^{2+} -dependent Ca_i^{2+} mobilization was abolished after overnight pre-exposure to pertussis toxin (300 ng mL^{-1}) and was insensitive to the phosphodiesterase inhibitor IBMX (0.2 mM), thereby demonstrating that $\text{G}_{i/o}$ -mediated inhibition of adenylyl cyclase was the major determinant of Ca_o^{2+} -stimulated suppression of cAMP levels in these experiments (not shown). HEK-293 cells were transiently co-transfected with a cAMP reporter construct and one of the four CaSR mutants, and studied by microfluorimetry as described in the Methods section. Samples of transfected cells were exposed to 1 μM forskolin to elevate intracellular cAMP levels followed by step-wise increments in Ca_o^{2+} from 0.5 to 10 mM.

HEK-293 cells transfected with the WTCaSR exhibited Ca_o^{2+} -dependent suppression of 1 μM forskolin-stimulated cAMP levels with an EC_{50} for Ca_o^{2+} of 1.7 ± 0.2 mM and a maximal 60% suppression of cAMP levels (Fig. 4). Two of the point mutations, F706A and L797A abolished Ca_o^{2+} -dependent cAMP suppression (Fig. 4). However, surprisingly, the Ca_o^{2+} -stimulated inhibitory responses were maintained in HEK-293 cells transfected with either the iL-3 point mutation E803A or the C-terminus truncation mutant R866X. In the case of R866X, there was no apparent change in the EC_{50} for Ca_o^{2+} . In the case of E803A, an apparent drop in EC_{50} for Ca_o^{2+} from 1.7 ± 0.2 to 0.9 ± 0.1 mM (Fig. 4) was not statistically significant ($P = 0.07$). The findings demonstrate that the molecular requirements for Ca_o^{2+} -stimulated CaSR-mediated inhibition of cAMP levels are clearly distinct from those required for the control of PI-PLC, Ca_i^{2+} mobilization and p $\text{ERK}_{1/2}$ and provide new insights into the nature of biased signalling.

4. Discussion

Within GPCR class C there is a sub-group of nutrient-sensing receptors that respond to both macronutrients, such as L-amino acids, as well as micronutrients, such as Ca^{2+} ions (review: [2]).

The CaSR is a key member of this receptor subgroup that plays diverse physiological roles. These include the feedback control of calcium homeostasis via cell-based mechanisms in the parathyroid, renal thick ascending limb, and bone [24], the modulation of tissue development and cell fate [7], and L-amino acid sensing mechanisms [25] and various other functions in the gastro-intestinal tract (review: [26]). This surprising pluripotency requires precise control over a large number of receptor-coupled signalling pathways, and, thus, mechanisms by which the receptor can select between pathways.

In the present study, we focused on Ca_o^{2+} -stimulated control of four key CaSR-mediated signalling pathways: PI-PLC, Ca_i^{2+} mobilization; ERK_{1/2} phosphorylation; and suppression of adenylyl cyclase, using key point mutants of CaSR iL-2 and iL-3, as well as a truncation mutant of the proximal C-terminus to assess the roles of these structural components in the selection of distinct signalling pathways. We used transient expression of the five different CaSR constructs in the present study to ensure that the cell context was identical in all cases. None of the mutants impaired either total or surface expression of the receptor, and all of them exhibited marked suppression of Ca_o^{2+} -stimulated PI-PLC (Figs. 1B and 2A) as reported previously [17,19]. Strikingly, we found that the C-terminal-proximal region is required for the activation of PI-PLC, Ca_i^{2+} mobilization and pERK_{1/2} but not for $G_{i/o}$ -dependent inhibition of adenylyl cyclase, as reported by the suppression of forskolin-stimulated elevations in cAMP levels. In addition, we observed important differences in the roles of key iL-2 and iL-3 residues in supporting signalling by distinct pathways. Thus, although F706 and L797 were required for both $G_{q/11}$ - and $G_{i/o}$ -dependent signalling, E803 was only required for $G_{q/11}$ and not $G_{i/o}$ -dependent signalling. The results indicate that distinct residues in these key intracellular regions of the CaSR are required by the mechanisms that engage specific pathways in response to Ca_o^{2+} -stimulation. See Table 2 for a summary of the outcomes.

All mutants markedly impaired Ca_o^{2+} -stimulated pERK_{1/2} as well as PI-PLC suggesting the existence of a common signalling mechanism downstream of $G_{q/11}$. Ca_o^{2+} -stimulated CaSR-mediated pERK_{1/2} was nearly abolished by the PI-PLC inhibitor, U73122, and also markedly suppressed following pre-treatment with pertussis toxin, which disables $G_{i/o}$ [15,27]. Thus, both $G_{q/11}$ -stimulated PI-PLC and $G_{i/o}$ appear to be required for pERK_{1/2}.

Surprisingly, there were notably lesser impacts of the three point mutants on Ca_i^{2+} mobilization when compared with their effects on IP₁ accumulation (Fig. 2B) and only the C-terminus truncation mutant R866X abolished Ca_o^{2+} -stimulated Ca_i^{2+} mobilization. Thus, the results suggest only a partial dependence of CaSR-mediated Ca_i^{2+} mobilization on PI-PLC. Other pathways that may contribute to CaSR-mediated Ca_i^{2+} mobilization include a $G_{12/13}$ -coupled pathway dependent on a Rho and Filamin-A-dependent interaction with the receptor's C-terminus [28]. Such a mechanism could explain how the C-terminal truncation mutant R866X abolished Ca_i^{2+} mobilization. G_{12} has also been reported to activate protein

phosphatase 2A [29], an enzyme that supports Ca_o^{2+} -stimulated dephosphorylation of CaSR residue T888 and, in turn, promotes stable elevations in Ca_i^{2+} [30].

Preliminary experiments investigating the effects of pre-treatment with pertussis toxin and of acute exposure to the broad-spectrum phosphodiesterase (PDE) inhibitor IBMX demonstrated that the suppressive effect of Ca_o^{2+} on forskolin-induced elevations in cAMP levels was dependent on $G_{i/o}$ -mediated inhibition of adenylyl cyclase and not PDE. Thus, the finding that F706A (iL-2) and L797A (iL-3) were resistant to Ca_o^{2+} -stimulated suppression of cAMP is consistent with the idea that both these residues are required for CaSR-mediated coupling to $G_{i/o}$ as well as $G_{q/11}$. However Ca_o^{2+} -stimulated suppression of cAMP levels was retained at apparently WT levels in the cases of the point mutant E803A (iL-3) and the C-terminus truncation mutant R866X, demonstrating the existence of distinct requirements for the activation of PI-PLC and inhibition of adenylyl cyclase. In addition, the finding that R866X abolished Ca_o^{2+} -stimulated Ca_i^{2+} mobilization but exhibited WT levels of Ca_o^{2+} -stimulated suppression of cAMP appears to exclude a role for Ca_i^{2+} -dependent inhibition of adenylyl cyclase in the present experiments in which forskolin was used to elevate cAMP levels, distinct from that reported previously for CaSR-expressing HEK-293 cells in which they were elevated by prostaglandin E₂ or isoproterenol [31].

The finding that CaSR-mediated coupling to the control of PI-PLC and adenylyl cyclase is dependent on distinct residues is consistent with findings on the signalling requirements of another class C GPCR, mGluR1, in which some iL-2 mutants, including T695A, K697A and S702A, selectively disabled PI-PLC activation, whereas others including P698A and the two residue deletion C694-T695, selectively impaired cAMP accumulation [32]. Similarly, deletion of the mGluR1 C-terminus selectively abolished $G_{q/11}$, but not $G_{i/o}$ -dependent signalling [33] as observed in the present study for the Ca_o^{2+} -stimulated CaSR (Fig. 4).

The C-terminus also plays important roles in coupling other class C GPCRs to specific G-protein-dependent signalling pathways [34]. For example, alternative splicing of mGluR-1 results in distinct G-protein coupling profiles based on differences in C-terminus sequences. Thus, mGluR-1 α with a longer C-terminus coupled efficiently to both $G_{q/11}$ and G_s , whereas mGluR-1 β with a shorter C-terminus coupled efficiently to $G_{q/11}$ but did not couple to G_s [35]. Furthermore, deletion of the mGluR-1 C-terminus selectively abolished $G_{q/11}$ -dependent but not $G_{i/o}$ -dependent signalling [33].

It is notable in the present study that where one or more of the iL-2, iL-3 or C-terminus mutants impaired CaSR-mediated stimulation of PI-PLC, Ca_i^{2+} mobilization, ERK_{1/2} phosphorylation, and/or inhibition of adenylyl cyclase, the primary effect was a reduction in the maximal response (E_{max}) rather than an increase in the EC₅₀ value for Ca_o^{2+} (see Figs. 2–4), as more commonly reported for mutations in human kindreds with familial hypocalciuric hypercalcemia (FHH) or neonatal severe primary hyperparathyroidism (NSHPT) (reviews: [36–38]). The finding that E_{max} was reduced is consistent with the idea that Ca_o^{2+} binding and Ca_o^{2+} -dependent changes in receptor conformation were normal in the extracellular VFT and Cys-rich domains, but that coupling of the activated receptor to its signalling apparatus in the dimeric heptahelical domains was defective as a result of impaired binding of partner proteins including G-proteins and enzymes.

In the present study we have identified CaSR residues in iL-2 and iL-3 as well as the proximal C-terminus that are required for Ca_o^{2+} -stimulated signalling, and demonstrated the existence of distinct requirements for the activation of PI-PLC and Ca_i^{2+} mobilization, and suppression of adenylyl cyclase. Further work is required to properly define the requirements of Ca_o^{2+} -stimulated pathways downstream of $G_{q/11}$, $G_{i/o}$ and $G_{12/13}$, and to assess the ligand-biased signalling requirements of physiologically and pharmacologically

Table 2

Impacts of mutations on Ca_o^{2+} -stimulated CaSR signalling. The inhibitory effects of the four mutants are summarized with respect to the wild-type CaSR for PI-PLC, pERK_{1/2}, Ca_i^{2+} mobilization, and inhibition of adenylyl cyclase (AC). '+++', indicates a WT response; '++' and '+' indicate moderately reduced or markedly reduced responses; '-' indicates abolition of the response.

	WT	F706	L797	E803	R866X
PI-PLC	+++	+	+	+	+
Ca_i^{2+} mobilisation	+++	++	++	++	-
pERK _{1/2}	+++	+	+	+	+
Inhibition of AC	+++	-	-	+++	+++

important agonists including divalent cations such as Mg^{2+} and Si^{2+} and organic polycations such as spermine, as well as modulators including L-amino acids and cinacalcet.

Acknowledgments

The project was supported by the NHMRC of Australia via Project Grant APP1026962 and Program Grant 519461. AC is an NHMRC Principal Research Fellow.

References

- [1] Conigrave, A.D. and Hampson, D.R. (2006) Broad-spectrum amino acid sensing by class 3 G-protein coupled receptors. *Trends Endocrinol. Metab.* 17, 398–407.
- [2] Conigrave, A.D. and Hampson, D.R. (2010) Broad-spectrum amino acid-sensing class C G-protein coupled receptors: molecular mechanisms, physiological significance and options for drug development. *Pharmacol. Ther.* 127, 252–260.
- [3] Khan, M.A. and Conigrave, A.D. (2010) Mechanisms of multimodal sensing by extracellular Ca^{2+} -sensing receptors: a domain-based survey of requirements for binding and signalling. *Br. J. Pharmacol.* 159, 1039–1050.
- [4] Leach, K., Sexton, P., Christopoulos, A. and Conigrave, A. (2014) Engineering biased signalling from the calcium-sensing receptor for the pharmacotherapy of diverse disorders. *Br. J. Pharmacol.* 171, 1142–1155.
- [5] Magno, A., Ward, B. and Ratajczak, T. (2011) The calcium-sensing receptor: a molecular perspective. *Endocr. Rev.* 32, 330.
- [6] Brown, E.M. and MacLeod, R.J. (2001) Extracellular calcium sensing and extracellular calcium signaling. *Physiol. Rev.* 81, 239–297.
- [7] Riccardi, D. and Kemp, P. (2012) The calcium-sensing receptor beyond extracellular calcium homeostasis: conception, development, adult physiology, and disease. *Annu. Rev. Physiol.* 74, 271–297.
- [8] Quinn, S.J., Ye, C.P., Diaz, R., Kifor, O., Bai, M., Vassilev, P. and Brown, E. (1997) The Ca^{2+} -sensing receptor: a target for polyamines. *Am. J. Physiol.* 273, C1315–C1323.
- [9] Conigrave, A.D., Quinn, S.J. and Brown, E.M. (2000) Cooperative multi-modal sensing and therapeutic implications of the extracellular Ca^{2+} -sensing receptor. *Trends Pharm. Sci.* 21, 401–407.
- [10] Mun, H., Franks, A., Culverston, E., Krapcho, K., Nemeth, E. and Conigrave, A. (2004) The Venus Fly Trap domain of the extracellular Ca^{2+} -sensing receptor is required for L-amino acid sensing. *J. Biol. Chem.* 279, 51739–51744.
- [11] Miedlich, S.U., Gama, L., Seuwen, K., Wolf, R.M. and Breitwieser, G.E. (2004) Homology modeling of the transmembrane domain of the human calcium sensing receptor and localization of an allosteric binding site. *J. Biol. Chem.* 279, 7254–7263.
- [12] Davey, A., Leach, K., Valant, C., Conigrave, A., Sexton, P. and Christopoulos, A. (2012) Positive and negative allosteric modulators promote biased signaling at the calcium-sensing receptor. *Endocrinology* 153, 1232–1241.
- [13] Leach, K., Wen, A., Davey, A., Sexton, P., Conigrave, A. and Christopoulos, A. (2012) Identification of molecular phenotypes and biased signaling induced by naturally occurring mutations of the human calcium-sensing receptor. *Endocrinology* 153, 4304–4316.
- [14] Leach, K., Wen, A., Cook, A., Sexton, P., Conigrave, A. and Christopoulos, A. (2013) Impact of clinically relevant mutations on the pharmacoregulation and signaling bias of the calcium-sensing receptor by positive and negative allosteric modulators. *Endocrinology* 154, 1105–1116.
- [15] Kifor, O., MacLeod, R.J., Diaz, R., Bai, M., Yamaguchi, T., Yao, T., Kifor, I. and Brown, E.M. (2001) Regulation of MAP kinase by calcium-sensing receptor in bovine parathyroid and CaR-transfected HEK293 cells. *Am. J. Physiol. Renal Physiol.* 280, F291–F302.
- [16] Hobson, S.A., Wright, J., Lee, F., McNeil, S.E., Bilderback, T. and Rodland, K.D. (2003) Activation of the MAP kinase cascade by exogenous calcium-sensing receptor. *Mol. Cell. Endocrinol.* 200, 189–198.
- [17] Chang, W., Chen, T.H., Pratt, S. and Shoback, D. (2000) Amino acids in the second and third intracellular loops of the parathyroid Ca^{2+} -sensing receptor mediate efficient coupling to phospholipase C. *J. Biol. Chem.* 275, 19955–19963.
- [18] Ray, K., Fan, G.F., Goldsmith, P.K. and Spiegel, A.M. (1997) The carboxyl terminus of the human calcium receptor. Requirements for cell-surface expression and signal transduction. *J. Biol. Chem.* 272, 31355–31361.
- [19] Chang, W., Pratt, S., Chen, T.H., Bourguignon, L. and Shoback, D. (2001) Amino acids in the cytoplasmic C terminus of the parathyroid Ca^{2+} -sensing receptor mediate efficient cell-surface expression and phospholipase C activation. *J. Biol. Chem.* 276, 44129–44136.
- [20] Bai, M. et al. (1996) Expression and characterization of inactivating and activating mutations in the human Ca^{2+} -sensing receptor. *J. Biol. Chem.* 271, 19537–19545.
- [21] Mun, H., Culverston, E., Franks, A., Collyer, C., Clifton-Bligh, R. and Conigrave, A. (2005) A double mutation in the extracellular Ca^{2+} -sensing receptor's Venus fly trap domain that selectively disables L-amino acid sensing. *J. Biol. Chem.* 280, 29067–29072.
- [22] Broadhead, G., Mun, H., Avlani, V., Jourdon, O., Church, W., Christopoulos, A., Delbridge, L. and Conigrave, A. (2011) Allosteric modulation of the calcium-sensing receptor by $[\gamma]$ -glutamyl peptides: inhibition of PTH secretion, suppression of intracellular cAMP levels and a common mechanism of action with L-amino acids. *J. Biol. Chem.* 286, 8786–8797.
- [23] van der Krogt, G.N.M., Ogink, J., Ponsioen, B. and Jalink, K. (2008) A comparison of donor-acceptor pairs for genetically encoded FRET sensors: application to the Epac cAMP sensor as an example. *PLoS ONE* 3, 1–9.
- [24] Brown, E. (2013) Role of the calcium-sensing receptor in extracellular calcium homeostasis. *Best Pract. Res. Clin. Endocrinol. Metab.* 27, 333–343.
- [25] Conigrave, A.D. and Brown, E.M. (2006) L-amino acid-sensing by calcium-sensing receptors: implications for GI physiology. *Am. J. Physiol.* 291, G753–G761.
- [26] Macleod, R. (2013) CaSR function in the intestine: hormone secretion, electrolyte absorption and secretion, paracrine non-canonical Wnt signaling and colonic crypt cell proliferation. *Best Pract. Res. Clin. Endocrinol. Metab.* 27, 385–402.
- [27] Avlani, V., Ma, W., Mun, H.-C., Leach, K., Delbridge, L., Christopoulos, A. and Conigrave, A. (2013) Calcium-sensing receptor-dependent activation of CREB phosphorylation in HEK-293 cells and human parathyroid cells. *Am. J. Physiol. Endocrinol. Metab.* 304, E1097–E1104.
- [28] Rey, O., Young, S.H., Yuan, J., Slice, L. and Rozengurt, E. (2005) Amino acid-stimulated Ca^{2+} oscillations produced by the Ca^{2+} -sensing receptor are mediated by a phospholipase C/inositol 1,4,5-trisphosphate-independent pathway that requires G12, Rho, filamin-A, and the actin cytoskeleton. *J. Biol. Chem.* 280, 22875–22882.
- [29] Kelly, P., Casey, P. and Meigs, T. (2007) Biologic functions of the G12 subfamily of heterotrimeric G proteins: growth, migration, and metastasis. *Biochemistry* 46, 6677–6687.
- [30] McCormick, W.D., Atkinson-Dell, R., Campion, K.L., Mun, H., Conigrave, A.D. and Ward, D.T. (2010) Increased receptor stimulation elicits differential calcium-sensing receptor T888 dephosphorylation. *J. Biol. Chem.* 285, 14170–14177.
- [31] Gerbino, A., Ruder, W.C., Curci, S., Pozzan, T., Zaccolo, M. and Hofer, A.M. (2005) Termination of cAMP signals by Ca^{2+} and $G(\alpha)_i$ via extracellular Ca^{2+} sensors: a link to intracellular Ca^{2+} oscillations. *J. Cell Biol.* 171, 303–312.
- [32] Francesconi, A. and Duvoisin, R. (1998) Role of the second and third intracellular loops of metabotropic glutamate receptors in mediating dual signal transduction activation. *J. Biol. Chem.* 273, 5615–5624.
- [33] Kammermeier, P. (2010) C-terminus deletion of metabotropic glutamate receptor 1 selectively abolishes coupling to Galphaq. *Eur. J. Pharmacol.* 627, 63–68.
- [34] Perroy, J., Gutierrez, G., Coulon, V., Bockaert, J., Pin, J. and Fagni, L. (2001) The C terminus of the metabotropic glutamate receptor subtypes 2 and 7 specifies the receptor signaling pathways. *J. Biol. Chem.* 276, 45800–45805.
- [35] Tateyama, M. and Kubo, Y. (2007) Coupling profile of the metabotropic glutamate receptor 1alpha is regulated by the C-terminal domain. *Mol. Cell. Neurosci.* 34, 445–452.
- [36] Hendy, G.N., D'Souza-Li, L., Yang, B., Canaff, L. and Cole, D.E.C. (2000) Mutations of the calcium-sensing receptor (CASR) in familial hypocalcaemic hypercalcaemia, neonatal severe hyperparathyroidism, and autosomal dominant hypocalcaemia. *Hum. Mutat.* 16, 281–296.
- [37] Tfelt-Hansen, J. and Brown, E. (2005) The calcium-sensing receptor in normal physiology and pathophysiology: a review. *Crit. Rev. Clin. Lab. Sci.* 42, 35–70.
- [38] Hannan, F. and Thakker, R. (2013) Calcium-sensing receptor (CaSR) mutations and disorders of calcium, electrolyte and water metabolism. *Best Pract. Res. Clin. Endocrinol. Metab.* 27, 359–371.